Inorg. Chem. **2003**, *42*, 8223–8229

"Nanoscale Zippers" in $Gd_5(Si_xGe_{1-x})_4$: Symmetry and Chemical Influences on the Nanoscale Zipping Action

Wonyoung Choe,[†,‡] A. O. Pecharsky,[§] Michael Wörle,[||] and Gordon J. Miller*[,†]

Department of Chemistry, Department of Materials Science and Engineering, and Ames Laboratory, U.S. Department of Energy, Iowa State University, Ames, Iowa 50011, and Laboratory of Inorganic Chemistry, ETH Hoenggerberg, HCI, CH-8093 Zürich, Switzerland

Received August 6, 2003

One critical parameter influencing the structural nature of the phase transitions in magnetocaloric materials $Gd_5(Si_xGe_{1-x})_4$ is the Si/Ge ratio ($x/1 - x$), because transition temperatures and structures depend crucially on this value. In this study, single-crystal X-ray diffraction indicates that Si and Ge atoms are neither completely ordered nor randomly mixed among the three crystallographic sites for these elements in these structures. Ge atoms enrich the T sites linking the characteristic slabs in these structures, while Si atoms enrich the T sites within them. Decomposition of the total energy into site and bond energy terms provides a rationale for the observed distribution, which can be explained by symmetry and electronegativity arguments. For any composition in $Gd_5(Si_xGe_{1-x})_4$, a structure map is presented that will allow for a rapid assessment of the specific structure type.

Introduction

Aside from the fascinating magnetic and electrical properties discovered in the $Gd_5(Si_xGe_{1-x})_4$ system such as the giant magnetocaloric effect,[1] colossal magnetostriction,[2] giant magnetoresistance,[3] spontaneous voltage generation,[4] and an unusual Hall effect,[5] one structural feature of $Gd_5(Si_xGe_{1-x})_4$ that has captured the attention of solid-state chemists is its remarkable ability to cleave or re-form the covalent bonds between pairs of (Si, Ge) atoms during the magnetically coupled, crystallographic phase transition for $x \leq 0.503$ in the vicinity of respective transition temperatures.[6,7] Across these transitions, the distances between pairs of (Si, Ge) atoms change by ca. 0.9 Å. Since the making and breaking of covalent bonds are reminiscent of the closing and opening action of a zipper, $Gd_5(Si_xGe_{1-x})_4$ can be considered as "nanoscale zippers" in the solid state.[7,8] The three "nanoscale zipper" structures observed in $Gd_5(Si_xGe_{1-x})_4$ at room temperature[9] are the Sm_5Ge_4-type[10] (orthorhombic, *Pnma*, $0 \leq x \leq 0.3$), the $Gd_5Si_2Ge_2$-type[9d] (monoclinic, $P112_1/a$, $0.43 \leq x \leq 0.503$), and the Gd_5Si_4-type[11] (orthorhombic, *Pnma*,

* To whom correspondence should be addressed. E-mail: gmiller@iastate.edu.
† Department of Chemistry, Iowa State University.
‡ Current address: Lawrence Livermore National Laboratory, L-418, 7000 East Ave., Livermore, CA 94550.
§ Department of Materials Science and Engineering and Ames Laboratory, Iowa State University.
|| Laboratory of Inorganic Chemistry, ETH Hoenggerberg.

(1) (a) Pecharsky, V. K.; Gschneidner, K. A., Jr. *Phys. Rev. Lett.* **1997**, *78*, 4494−4497. (b) Pecharsky, V. K.; Gschneidner, K. A., Jr. *Appl. Phys. Lett.* **1997**, *70*, 3299−3301. (c) Pecharsky, V. K.; Gschneidner, K. A., Jr. *J. Magn. Magn. Mater.* **1997**, *167*, L179−184. (d) Giguere, A.; Foldeaki, M.; Ravi Gopal, R.; Bose, T. K.; Frydman, A. *Phys. Rev. Lett.* **1999**, *83*, 2262. (e) Gschneidner, K. A., Jr.; Pecharsky, V. K.; Brück, E.; Duijin, H. G. M.; Levin, E. M. *Phys. Rev. Lett.* **2000**, *85*, 4190. (f) Pecharsky, A. O.; Gschneidner, K. A., Jr.; Pecharsky, V. K. *J. Appl. Phys.* **2003**, *93*, 4722.
(2) (a) Morellon, L.; Blasco, J.; Algarabel, P. A.; Ibara, M. R. *Phys. Rev. B* **2000**, *62*, 1022. (b) Morellon, L.; Algarabel, P. A.; Ibara, M. R.; Blasco, J. *Phys. Rev. B* **1998**, *58*, R14721. (c) Magen, C.; Morellon, L.; Algarabel, P. A.; Marquina, C.; Ibarra, M. R. *J. Phys.: Condens. Matter* **2003**, *15*, 2389.
(3) (a) Morellon, L.; Stankiewicz, J.; Gracia-Landa, B.; Algarabel, P. A.; Ibara, M. R. *Appl. Phys. Lett.* **1998**, *73*, 3462. (b) Levin, E. M.; Pecharsky, V. K.; Gschneidner, K. A., Jr. *Phys. Rev. B* **1999**, *60*, 7993. (c) Levin, E. M.; Pecharsky, V. K.; Gschneidner, K. A., Jr. *J. Magn. Magn. Mater.* **2000**, 210, 181.
(4) Levin, E. M.; Pecharsky, V. K.; Gschneidner, K. A., Jr. *Phys. Rev.* **2001**, *B63*, 174110.
(5) Stankiewicz, J.; Morellon, L.; Algarabel, P. A.; Ibara, M. R. *Phys. Rev.* **2000**, *B61*, 12651.
(6) Choe, W.; Pecharsky, V. K.; Pecharsky, A. O.; Gschneidner, K. A., Jr.; Young, V. G., Jr.; Miller, G. J. *Phys. Rev. Lett.* **2000**, *84*, 4617.
(7) Choe, W.; Miller, G. J.; Meyers, J.; Chumbley, S.; Pecharsky, A. O. *Chem. Mater.* **2003**, *15*, 1413.
(8) For examples of other "molecular zippers", see: Iodanidis, L.; Kanatzidis, M. G. *J. Am. Chem. Soc.* **2000**, *122*, 8319 and references therein.
(9) Room-temperature X-ray powder studies on the $Gd_5(Si_xGe_{1-x})_4$ system include the following: (a) Liu, Q. L.; Rao, G. H.; Yang, H. F.; Liang, J. K. *J. Alloys Compd.* **2001**, *325*, 50. (b) Pecharsky, A. O.; Gschneidner, K. A.; Pecharsky, V. K.; Schindler, C. E. *J. Alloys Compd.* **2002**, *338*, 126. (c) Liu, Q. L.; Rao, G. H.; Liang, J. K. *Rigaku J.* **2001**, *18*, 46−50. (d) Pecharsky, V. K.; Gschneidner, K. A., Jr. *J. Alloys Compd.* **1997**, *260*, 98.
(10) Holtzberg, F.; Gambino, R. J.; McGuire, T. R. *J. Phys. Chem. Solids* **1967**, *28*, 2283.

10.1021/ic034941z CCC: $25.00
Published on Web 11/07/2003

Table 1. Crystallographic Data for $Gd_5(Si_xGe_{1-x})_4$ at 292 K

	x			
param	0	0.11	0.32	0.46
cryst system	orthorhombic	orthorhombic	orthorhombic	monoclinic
space group	*Pnma* (No.62)	*Pnma* (No. 62)	*Pnma* (No. 62)	$P112_1/a$ (No. 14)
a, Å	7.697(1)	7.689(1)	7.665(1)	7.587(1)
b, Å	14.831(1)	14.823(2)	14.809(2)	14.798(2)
c, Å	7.785(1)	7.777(1)	7.769(1)	7.790(3)
γ, deg	90	90	90	93.265(2)
V, Å^3	888.7(2)	886.4(2)	882.0(2)	872.2(2)
R_1 [$I > 2\sigma(I)$]	0.0287	0.0597	0.0421	0.0419
wR2 [$I > 2\sigma(I)$]	0.0739	0.2042	0.1064	0.0754
R_1 (all data)	0.0394	0.0641	0.0540	0.0836
wR2 (all data)	0.0828	0.2077	0.1128	0.0829

$0.575 < x \leq 1$). Each structure is constructed from two-dimensional $^{\infty}_{2}[Gd_5T_4]$ slabs,[6] where T represents Si or Ge, but their differences arise by how these slabs stack with respect to one another.[6,7]

One of the crucial variables that can induce such drastic structural transformation in the $Gd_5(Si_xGe_{1-x})_4$ system is the Si/Ge ratio.[12] Interestingly, Si and Ge atoms in $Gd_5(Si_xGe_{1-x})_4$ are neither completely ordered nor randomly mixed, based on the single-crystal data of $Gd_5Si_2Ge_2$[6] and $Gd_5Si_{1.5}Ge_{2.5}$.[7] The distribution of Si and Ge atoms at an atomic scale becomes a latest, critical issue of this series.[7] Previous studies on the $Gd_5(Si_xGe_{1-x})_4$ system primarily focused on the Si/Ge ratio of the bulk polycrystalline alloys.[9] We are now concerned with the Si and Ge occupation at each crystallographic site because these (Si,Ge) atoms are the ones that break, re-form, or sustain the covalent bonds during the phase transition. The T−T dimers can be homonuclear Si−Si and Ge−Ge or heteronuclear Si−Ge, with the ratio among the three different dimer species varying as the bulk Si/Ge ratio changes.[13] However, the role of different dimer species on the structural evolution of this series of compounds has yet to be addressed. To study this problem experimentally, single-crystal X-ray diffraction of the $Gd_5(Si_xGe_{1-x})_4$ series is a prerequisite.[14] The site occupation data extracted from the single-crystal X-ray diffraction studies do provide information for further detailed theoretical studies to explain why the dimers in certain slabs break while others do not. However, the complete story necessarily requires local probes of chemical structure. Here we report single-crystal X-ray diffraction studies on the Ge-rich region of $Gd_5(Si_xGe_{1-x})_4$, thereby monitoring any changes in atomic coordinates as well as Si/Ge occupation at each T site across the $Gd_5(Si_xGe_{1-x})_4$ series. While compiling the cell parameter data in the $Gd_5(Si_xGe_{1-x})_4$ system, we note that a simple plot of *c/a* ratio vs *b/a* ratio can effectively separate three known structure types in $Gd_5(Si_xGe_{1-x})_4$. This plot can be used as a structure sorting map and will allow rapid assessment of the three structure types in the $Gd_5(Si_xGe_{1-x})_4$ and its related systems.

Experimental and Theoretical Methods

Synthesis. The $Gd_5(Si_xGe_{1-x})_4$ samples, where $x = 0$, 0.11, 0.32, and 0.46, were prepared by arc-melting its constituent elements in an argon atmosphere on a water-cooled copper hearth. The starting materials were high purity Gd (99.99 wt %, Materials Preparation Center of the Ames Laboratory), Si (99.9999+ wt %, CERAC, Inc.), and Ge (99.9999 wt %, CERAC, Inc.). Each alloy was remelted several times from both sides of the arc-melted button to ensure homogeneity. Single crystals were selected from the as-cast sample. Final products were analyzed using semiquantitative energy dispersive spectroscopy (EDS) attached to a scanning electron microscope (SEM). The differences between starting and measured sample compositions were within 3 at. %. Further annealing of the $Gd_5(Si_xGe_{1-x})_4$ samples leads to formation of $Gd(Si_xGe_{1-x})$ and $Gd_5(Si_xGe_{1-x})_3$ as well as crystals of poorer quality for single-crystal X-ray diffraction experiments.[7]

X-ray Crystallography. X-ray diffraction data were collected at 292 K using a Bruker CCD-1000, three-circle diffractometer with Mo Kα radiation ($\lambda = 0.710\ 73$ Å) and a detector-to-crystal distance of 5.08 cm on 2−3 crystal specimens for each composition. Data were collected in at least a quarter hemisphere and were harvested by collecting three sets of frames with 0.3° scans in ω for an exposure time of 10−20 s/frame. The range of 2θ extended from 3.0 to 56.0°. The reflections were extracted from the frame data using the SMART program[15] and then integrated using the SAINT program.[15] Data were corrected for Lorentz and polarization effects. Absorption corrections using SADABS[15] were based on fitting a function to the empirical transmission surface as sampled by multiple equivalent reflections. Unit cell parameters were indexed by peaks obtained from 90 frames of reciprocal space images and then refined using all observed diffraction peaks after data integration. The structure solution was obtained by direct methods and refined by full-matrix least-squares refinement of F_o^2 using the Bruker SHELXTL package.[15] Table 1 lists crystallographic data

(11) Smith, G. S.; Johnson, Q.; Tharp, A. G. *Acta Crystallogr.* **1967**, *22*, 269.

(12) Other known variables which could induce a structure transition include temperature,[6,7] magnetic field,[12a,b] pressure,[12a,c] and valence electron concentration (VEC):[12d] (a) Morellon, L.; Algarabel, P. A.; Ibarra, M. R.; Blasco, J.; García-Landa, B. *Phys. Rev. B* **1998**, R14721. (b) Tang, H.; Pecharsky, A. O.; Schlagel, D. L.; Lograsso, T. A.; Pecharsky, V. K.; Gschneidner, K. A., Jr. *J. Appl. Phys.* **2003**, *93*, 8298. (c) Pecharsky, V. K.; Gschneidner, K. A., Jr. *Adv. Mater.* **2001**, *13*, 683. (d) Mozharivskij, Y.; Choe, W.; Miller, G. J. *J. Am. Chem. Soc.*, submitted for publication.

(13) For example, one can generate a series of Gd_5Si_4-type structures with a stoichiometry of $Gd_5(Si_2Ge_2)$ in numerous ways. Some examples are $Gd_5[(Si-Si)(Ge-Ge)]$, $Gd_5[(Si-Ge)_2]$, and $Gd_5[(Si-Ge)_{2/3}(Si-Si)_{2/3}(Ge-Ge)_{2/3}]$, where the atom pairs in the brackets indicate dimer pairs in the Gd_5Si_4-type structures.

(14) X-ray single-crystal diffraction is far superior to X-ray powder diffraction to determine the occupation in mixed atomic sites. Although there are powder refinements reported on various $Gd_5(Si_xGe_{1-x})_4$, all of these refinements were based on the assumption that all T sites are occupied by statistical mixtures of Si and Ge atoms. See ref 9d and the following: Morellon, L.; Blasco, J.; Algarabel, P. A.; Ibarra, M. R. *Phys. Rev.* **2000**, *B62*, 1022.

(15) *SMART, SAINT, SHELXTL, and SADABS*; Bruker Analytical X-ray Instruments Inc.: Madison, WI, 2001.

Table 2. Positional Coordinates, Site Occupancies, and Isotropic Displacement Parameters for $Gd_5(Si_xGe_{1-x})_4$ at 292 K

x		*x/a*	*y/b*	*z/c*	occ[a]	U_{eq},[b] Å^2
0	Gd1	0.97585(10)	0.39988(5)	0.17788(10)	1	0.0077(3)
	Gd2	0.62314(9)	0.38328(5)	0.83851(9)	1	0.0065(3)
	Gd3	0.20994(13)	3/4	0.49913(13)	1	0.0058(4)
	T1	0.78241(19)	0.45610(11)	0.5329(2)	1	0.0072(4)
	T2	0.0823(3)	3/4	0.1129(3)	1	0.0073(6)
	T3	0.3261(3)	3/4	0.8654(3)	1	0.0071(6)
0.11	Gd1	0.9767(1)	0.39996(5)	0.1784(1)	1	0.0157(3)
	Gd2	0.6237(1)	0.38310(5)	0.8382(1)	1	0.0142(3)
	Gd3	0.2091(1)	3/4	0.4993(1)	1	0.0143(3)
	T1	0.7824(2)	0.4560(1)	0.5329(2)	0.950(10)	0.0156(6)
	T2	0.0816(3)	3/4	0.1122(3)	0.789(14)	0.0130(8)
	T3	0.3244(4)	3/4	0.8659(3)	0.873(14)	0.0149(8)
0.32	Gd1	0.9789(1)	0.40015(5)	0.1790(1)	1	0.0083(2)
	Gd2	0.6251(1)	0.38272(5)	0.8374(1)	1	0.0071(2)
	Gd3	0.2077(1)	3/4	0.4996(1)	1	0.0073(3)
	T1	0.7843(2)	0.4565(1)	0.5336(2)	0.752(6)	0.0077(6)
	T2	0.0809(3)	3/4	0.1109(3)	0.588(8)	0.006(1)
	T3	0.3211(3)	3/4	0.8672(4)	0.649(8)	0.0082(8)
0.46	Gd1A	0.99423(13)	0.40126(8)	0.18074(13)	1	0.0097(3)
	Gd1B	0.98277(13)	0.90111(8)	0.81812(13)	1	0.0101(3)
	Gd2A	0.64324(13)	0.38121(7)	0.83679(13)	1	0.0089(3)
	Gd2B	0.32985(13)	0.87798(7)	0.17734(13)	1	0.0089(3)
	Gd3	0.17551(15)	0.74650(8)	0.50549(13)	1	0.0092(3)
	T1A	0.7935(4)	0.4572(2)	0.5362(4)	0.637(13)	0.0099(10)
	T1B	0.1548(4)	0.9593(2)	0.4704(4)	0.603(12)	0.0111(10)
	T2	0.0475(4)	0.7513(3)	0.1084(4)	0.436(12)	0.0115(13)
	T3	0.2923(4)	0.7517(2)	0.8686(4)	0.478(12)	0.0085(11)

[a] All T1, T2, and T3 atomic sites are fully occupied with Si and Ge atoms. Only Ge occupations are listed. [b] Anisotropic thermal displacement parameters can be received from the authors upon request.

for the specimen from each sample showing the best quality of refinement, and Table 2 shows the corresponding atomic coordinates.

Electronic Structure Calculations. Tight-binding, linear muffin-tin orbital (TB-LMTO) electronic band structure calculations in the atomic sphere approximation (ASA) were carried out for various models of $Gd_5Si_2Ge_2$ (discussed in a subsequent section) using the LMTO47 program.[16] Exchange and correlation were treated in a local density approximation. All relativistic effects except spin−orbit coupling were taken into account using a scalar relativistic approximation. The radii of the Wigner−Seitz (WS) spheres were obtained by requiring the overlapping potential to be the best possible approximation to the full potential according to an automatic procedure—no empty spheres were necessary.[17] The WS radii determined by this procedure for the atoms in $Gd_5Si_2Ge_2$ are 1.847−2.053 Å for Gd, 1.541 Å for the T1 position, and 1.505 Å for the T2 and T3 positions. The basis set included Gd 6s, 6p, and 5d orbitals, Si 3s, 3p, and 3d orbitals, and Ge 4s, 4p, and 4d orbitals. The Gd 4f orbitals were treated as core functions with seven valence electrons. Furthermore, the Si 3d and Ge 4d orbitals were treated by the Löwdin downfolding technique.[16] The **k**-space integrations to determine the total valence electron energies and crystal Hamiltonian orbital populations[18] (COHP) were performed by the tetrahedron method using between 32 and 50 **k**-points in the irreducible wedges of the appropriate unit cells.

Results and Discussion

Structures. At room temperature, the $Gd_5(Si_xGe_{1-x})_4$ structures adopt the orthorhombic Sm_5Ge_4-type for $x = 0$, 0.11, and 0.32 and the monoclinic $Gd_5Si_2Ge_2$-type for $x = 0.46$ (Figure 1). Low-temperature structures, i.e., below the corresponding transition temperatures, are all of the Gd_5Si_4-type.[19] One notable point is that coordinates of the individual atomic sites do not change significantly in a given structure

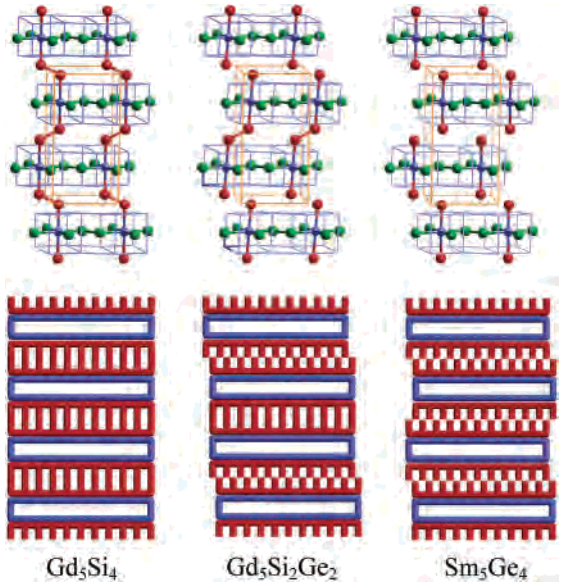

Figure 1. Three nanoscale zipper structures in $Gd_5(Si_xGe_{1-x})_4$ observed at room temperature: (left) orthorhombic Gd_5Si_4-type; (middle) monoclinic $Gd_5Si_2Ge_2$-type; (right) orthorhombic Sm_5Ge_4-type. The top three ball-and-stick representations highlight the Gd3 (blue), T1 (red), T2 (green), and T3 (green) sites. The Gd1 and Gd2 network in each slab is shown as the blue "lattice".

(16) (a) Andersen, O. K. *Phys. Rev. B* **1975**, *B12*, 3060. (b) Andersen, O. K.; Jepsen, O. *Phys. Rev. Lett.* **1984**, *53*, 2571. (c) Andersen, O. K.; Jepsen, O.; Glötzel, D. In *Highlights of Condensed-Matter Theory*; Bassani, F., Fumi, F., Tosi, M. P., Eds.; North-Holland: New York, 1985. (d) Andersen, O. K. *Phys. Rev. B* **1986**, *B34*, 2439.

(17) Jepsen, O.; Andersen, O. K. *Z. Phys. B* **1995**, *97*, 35.

(18) Dronskowski, R.; Blöchl, P. *J. Phys. Chem.* **1993**, *97*, 8617.

type as can be seen in Table 2, regardless of the Si content. This cannot be seen easily in previous X-ray powder diffraction patterns.[20] As mentioned in the Introduction, the critical difference between the Sm_5Ge_4-type and the $Gd_5Si_2Ge_2$-type is how the $^{\infty}_{2}[Gd_5T_4]$ slabs are connected: either by dimers or nonbonded, isolated "monomers". Figure 1 shows two kinds of T−T dimers, e.g. T2−T3 dimers in the slabs and T1−T1 dimers between the slabs. The T2−T3 interatomic distances are slightly dependent on the Si/Ge ratio and range from 2.63 to 2.68 Å as the Ge content increases,[21] which are ca. 5% longer than similar distances in other tetrelide compounds[22] containing 3^2434 nets of metals, e.g., the U_3Si_2-type, the Sm_5Ge_4-type, and the Cr_5B_3-type tetrelides.[23] Some examples include 2.525(3) Å for Gd_2MgGe_2,[24a] 2.513(3) Å for Gd_2InGe_2,[24b] 2.537(2) Å for La_2InGe_2,[24c] 2.620(6) Å for Hf_5Ge_4,[25] 2.5292(3) Å for Sr_5Ge_3,[26a] 2.530(4) Å for $Sr_5Si_{1.7}Ge_{1.3}$,[26b] 2.471(6) Å for $Sr_5Si_{2.87}Ge_{0.13}$,[26b] and 2.474(4) Å for Sr_5Si_3.[26c] On the other hand, in $Gd_5(Si_xGe_{1-x})_4$, as the Si content increases, it is remarkable to see that half of the monomers (T1−T1; 3.5−3.6 Å) in the Sm_5Ge_4-type becomes dimers (T1A−T1A; 2.5−2.7 Å) in the $Gd_5Si_2Ge_2$-type while the other half remains as monomers (T1B−T1B; 3.5−3.6 Å). Therefore, the interslab distance between (Si,Ge)−(Si,Ge) pairs can be viewed as a signature for distinguishing the three structure types, i.e., 2.6 Å for the Gd_5Si_4-type, alternating 2.6 and 3.5 Å for the $Gd_5Si_2Ge_2$-type, and 3.5 Å for the Sm_5Ge_4-type. The structural transition from the Sm_5Ge_4-type to the $Gd_5Si_2Ge_2$-type is a rare example of a sequential reduction−oxidation reaction in the solid state.[7]

Si/Ge Occupation and Bond Breaking. Figure 2 illustrates the Ge occupation in each T site in $Gd_5(Si_xGe_{1-x})_4$ as a function of x. The Si and Ge atoms occupy each T site in a nonstatistical fashion as was already seen in $Gd_5Si_2Ge_2$[6] and $Gd_5Si_{1.5}Ge_{2.5}$.[7] For all x values, Ge atoms prefer the T1 site over the T2 or T3 sites. It is also interesting to see that

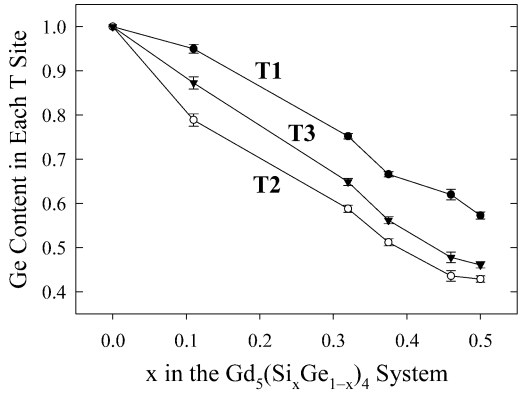

Figure 2. Ge occupation in each T site in $Gd_5(Si_xGe_{1-x})_4$ as a function of x. The data at $x = 0.375$ and 0.5 are respectively from refs 7 and 6. For the monoclinic structures at $x = 0.46$ and 0.5, T1A and T1B occupations are averaged.

the T3 site is always higher in Ge content than the T2 site, although the coordination environments are quite similar. To explain the observed phenomena, two issues are important:

(1) What influences the distribution of Si and Ge atoms among the various T sites, and

(2) why do T2−T3 dimers stay intact while T1−T1 dimers break as the Ge concentration increases?

These issues are related to both the chemical and symmetry aspects of the site preference problem in chemical structures,[27] which we address through electronic structure calculations.

We examined five model structures with a stoichiometry of $Gd_5Si_2Ge_2$ in its low-temperature form, i.e., the Gd_5Si_4-type: model **I** (space group *Pnma*) contains 100% Ge on T1 sites and 100% Si on both T2 and T3 sites; models **IIa** ($P112_1/a$), **IIb** ($P2_1ma$), and **IIc** ($Pn2_1a$) have 50% Si and 50% Ge on the T1 sites, Ge on the T2 sites, and Si on the T3 sites; model **III** has 100% Si on T1 sites and 100% Ge on both T2 and T3 sites. For all model **II** structures, the T2−T3 dimers are heteronuclear. Model **IIa** contains 50% Si−Si and 50% Ge−Ge dimers at the T1−T1 positions, whereas models **IIb,c** involve only heteronuclear Si−Ge dimers at the T1−T1 sites. Table 3 summarizes important results from the TB−LMTO−ASA calculations relevant to the coloring of Si and Ge in $Gd_5Si_2Ge_2$. Model **I** is most energetically stable, followed by **IIa−c** (ca. 0.069 eV/formula unit) and **III** (0.088 eV/formula unit). The lowest energy model **I** shows the trend found in our diffraction experiments, as this model has Ge atoms between the slabs in the T1 positions and Si atoms within the slabs in the T2 and T3 sites. However, we do not see a complete segregation of Ge and Si in any diffraction experiment on $Gd_5(Si_xGe_{1-x})_4$, which can be attributed to the entropy component of the free energy. For the $Gd_5Si_2Ge_2$ example, the free energy can be approximated by the following expression:

$$A(T) = E(f_I,f_{II},f_{III}) - TS(f_I,f_{II},f_{III})$$
$$= f_{II}\epsilon_{II} + f_{III}\epsilon_{III} + kT(f_I \ln f_I + f_{II} \ln f_{II} + f_{III} \ln f_{III})$$

Here f_I, f_{II}, and f_{III} represent the fractions of models **I−III**

(19) The low-temperature phases of all $Gd_5(Si_xGe_{1-x})_4$ structures with $x < 0.43$ belong to the Gd_5Si_4-type.[9] It is also known that all ferromagnetic phases have the Gd_5Si_4 type. See: Levin, E. M.; Pecharsky, V. K.; Gschneidner, K. A., Jr.; Miller, G. J. *Phy. Rev. B* **2001**, *64*, 235103.

(20) The $Gd_5(Si_xGe_{1-x})_4$ system has a two-phase region at $0.31 < x < 0.43$ and $0.503 < x < 0.575$. For this reason the powder refinements in those regions are not reliable.[9b]

(21) (a) T2−T3 dimer distances are 2.682(3) Å for Gd_5Ge_4, 2.675(4) Å for $Gd_5(Si_{0.11}Ge_{0.89})_4$, 2.641(4) Å for $Gd_5(Si_{0.32}Ge_{0.68})_4$, 2.626(4) Å for $Gd_5(Si_{0.4}Ge_{0.6})_4$,[7] 2.632(4) Å for $Gd_5(Si_{0.46}Ge_{0.54})_4$, and 2.623(4) Å for $Gd_5(Si_{0.5}Ge_{0.5})_4$.[6] (b) T1A−T1A dimer distances for the monoclinic phases are 2.739(4) Å for $Gd_5(Si_{0.46}Ge_{0.54})_4$ and 2.614(5) Å for $Gd_5(Si_{0.5}Ge_{0.5})_4$.[6] It is noteworthy that the T1A−T1A distance found in $Gd_5(Si_{0.46}Ge_{0.54})_4$, 2.739(7) Å, is rather long compared with typical T1−T1 dimer distances.

(22) Tetrelide is a general name for compounds that contain group IV elements such as C, Si, Ge, Sn, and Pb.

(23) Hyde, B. G.; Andersson, S. *Inorganic Crystal Structures*; Wiley: New York, 1989; p 290.

(24) U_3Si_2-type compounds: (a) Choe, W.; Levin, E. M.; Miller, G. J. *J. Alloys Compd.* **2001**, *329*, 121. (b) Choe, W.; Miller, G. J. Unpublished results. (c) Zaremba, V. I.; Stepien-Damm, A.; Nichiporuk, G. P.; Tyvanchuk, Yu. B.; Kalychak, Ya. M. *Kristallografiya* **1998**, *43*, 13.

(25) Zhao, J. T.; Parthé, E. *J. Less-Common Met.* **1990**, *162*, L27.

(26) Cr_5B_3-type compounds: (a) Nesper, R.; Zürcher, F. *Z. Kristallogr.-New Cryst. Struct.* **1999**, *214*, 21. (b) Zürcher, F. Ph.D. Dissertation, ETH, 1998. (c) Nesper, R.; Zürcher, F. *Z. Kristallogr.-New Cryst. Struct.* **1999**, *214*, 19. See also: Leon-Escamilla, E. A.; Corbett, J. D. *J. Solid State Chem.* **2001**, *159*, 149.

(27) Miller, G. J. *Eur. J. Inorg. Chem.* **1998**, 523.

Table 3. TB−LMTO−ASA Results from Five Different Structural Models of $Gd_5Si_2Ge_2$[a]

	model				
	I	**IIa**	**IIb**	**IIc**	**III**
tot. energy, eV	0	0.069	0.069	0.069	0.088
		Integrated COHP (eV)			
T1−T1	−1.928	-1.927^{Ge-Ge} -1.979^{Si-Si}	−1.954	−1.955	**−1.975**
T2−T3	**−2.191**	−2.179	−2.179	−2.179	−2.171
Gd1−Ge	**−1.089**	−1.038	−1.035	−1.035	−0.990
Gd1−Si	−1.030	−1.069	−1.071	−1.071	**−1.115**
Gd2−Ge	**−1.376**	−1.333	−1.332	−1.332	−1.209
Gd2−Si	−1.245	−1.277	−1.279	−1.279	**−1.403**
Gd3−Ge	−1.033	−1.052	−1.055	−1.051	**−1.192**
Gd3−Si	−1.196	**−1.240**	**−1.237**	**−1.241**	−1.068
S(T−T)	−4.119	−4.132	−4.133	−4.134	**−4.146**
S(Gd1−T)	**−7.446**	−7.390	−7.389	−7.389	−7.430
S(Gd2−T)	**−7.863**	−7.830	−7.833	−7.833	−7.836
S(Gd3−T)	−6.850	−6.876	−6.876	−6.876	**−6.904**
S(Gd−T)	**−37.468**	−37.316	−37.320	−37.320	−37.436
S(all)	**−41.587**	−41.448	−41.453	−41.454	−41.582

Electron Occupation Numbers

	model							
	I	**IIa**		**IIb**		**IIc**		**III**
T1	Ge	Ge	Si	Ge	Si	Ge	Si	Si
*n*s	1.39	1.39	1.32	1.38	1.33	1.38	1.33	1.32
*n*p	2.23	2.23	2.28	2.23	2.28	2.23	2.28	2.28
*n*d	0.13	0.13	0.17	0.13	0.17	0.13	0.17	0.17
T2	Si	Ge		Ge		Ge		Ge
*n*s	1.30	1.36		1.36		1.36		1.36
*n*p	2.32	2.27		2.26		2.26		2.26
*n*d	0.17	0.13		0.13		0.13		0.13
T3	Si	Si		Si		Si		Ge
*n*s	1.29	1.29		1.29		1.29		1.36
*n*p	2.21	2.21		2.21		2.21		2.15
*n*d	0.16	0.16		0.16		0.16		0.12
Gd1								
6s	0.60	0.60		0.60		0.60		0.60
6p	0.81	0.81		0.81		0.81		0.81
5d	2.03	2.03		2.03		2.03		2.03
Gd2								
6s	0.49	0.49		0.49		0.49		0.49
6p	0.61	0.61		0.61		0.61		0.61
5d	1.86	1.86		1.86		1.86		1.86
Gd3								
6s	0.61	0.61		0.61		0.61		0.61
6p	0.85	0.85		0.85		0.85		0.85
5d	1.80	1.80		1.80		1.80		1.80
$\Sigma q(T)\epsilon_{nl}$	**−6.6974**	−6.6888		−6.6849		−6.6849		−6.6799
$\Sigma q(Gd)\epsilon_{nl}$	−5.4858	−5.4858		−5.4858		−5.4858		−5.4858
$\Sigma q(all)\epsilon_{nl}$	**−12.1832**	−12.1746		−12.1707		−12.1707		−12.1657

[a] The orbital energies used in the calculation of site energy terms are a follows: Ge, $\epsilon_{4s} = -0.737$ eV, $\epsilon_{4p} = -0.310$ eV, $\epsilon_{4d} = -0.294$ eV; Si, $\epsilon_{3s} = -0.662$ eV, $\epsilon_{3p} = -0.304$ eV, $\epsilon_{3d} = -0.295$ eV. The specific orbital energies for Gd are available from the author. Values in boldface indicate the lowest value.

constituting the total system (therefore, $f_I + f_{II} + f_{III} = 1$) and ϵ_{II} and ϵ_{III} represent the total energies of models **II** and **III** relative to model **I** (i.e., $\epsilon_I = 0$). Due to the constraint on the fractions of each model, the free energy, $A(T)$, can be plotted as a contour map with respect to two fractions, f_I and f_{II}. Figure 3 illustrates these plots for a calculation at low temperature ($T = 500$ K) and at high temperature ($T = 2000$ K). At high temperature, the minimum free energy value occurs for the fractions $f_I = 0.40$, $f_{II} = 0.31$, and $f_{III} = 0.29$, which gives the T1 site occupancy as $f_{Ge} = 0.56$ and $f_{Si} = 0.44$. This result is in excellent agreement with experiment.[6] At the lower temperature, we find the minimum value for $f_I = 0.59$, $f_{II} = 0.11$, and $f_{III} = 0.30$, which gives the T1 site occupancy as $f_{Ge} = 0.70$ and $f_{Si} = 0.30$.

When electronic energies are calculated using a tight-binding scheme, the contribution from the valence electrons to these energies can be divided into two terms: a site energy term; a bond energy term.[27,28] Within the TB−LMTO−ASA method, we can examine the contribution from the bond energy term by calculating the crystal orbital Hamiltonian population (integrated COHP values).[18] The results for T1−T1 and T2−T3 dimers as well as for Gd−Ge and Gd−Si pairs are summarized in Table 3. Note that there is

(28) The competition between the site energy and the bond energy can be seen in structures such as $LnAu_xAl_{4-x}$ ($0.75 \le x \le 2$) and $AEZn_2Al_2$ (Ln = La−Tb; AE = Ca, Sr, Ba). See: Miller, G. J.; Lee, C.-S.; Choe, W. *Highlights in Inorganic Chemistry*; Meyer, G., Naumann, D., Wesemann, L., Eds.; Wiley-VCH: Weinheim, Germany, 2002; p 21.

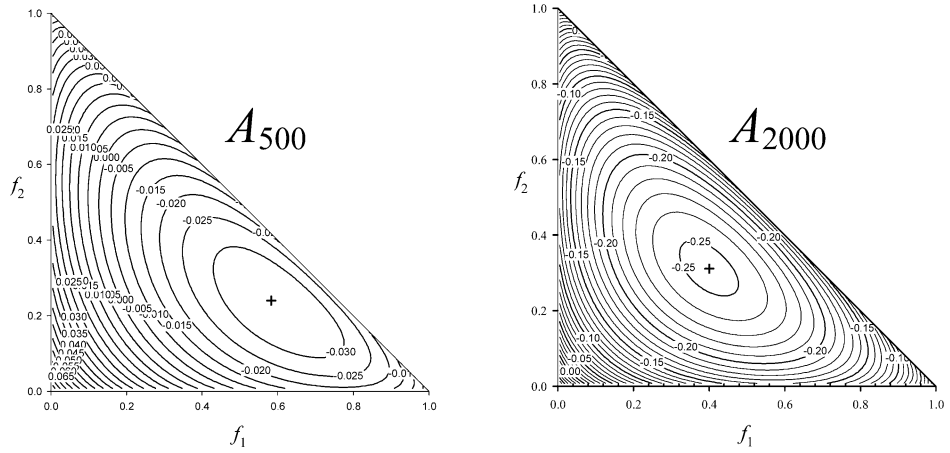

Figure 3. Contour plots of free energy, $A(T)$, plotted as a function of the fractions of models **I** (f_I) and **II** (f_{II}). For these two plots, $T = 500$ K (top) and 2000 K (bottom). The free energy minimum is marked by a cross.

very little difference between models **I** and **III** for the sum of T−T and Gd−T integrated COHPs, with just a slight preference for model **I** (by 0.005 eV/formula unit) due to Gd1−T and Gd2−T interactions. This indicates that even the two extreme cases of **I** and **III** are both plausible in terms of bond energy. Furthermore, we see that the T1−T1 bonds show consistently lower integrated COHP values than the T2−T3 bonds, which indicates a lower bond order for these T1−T1 interactions. Also, the integrated COHP values decrease from Si−Si to Si−Ge to Ge−Ge, in agreement with the dissociation energies for Ge−Ge (186 kJ/mol) and Si−Si (225 kJ/mol) dimers. Analysis of the site energy term from the valence electrons involves summing up the product of the atomic orbital charges and the corresponding orbital energy, which is summarized at the bottom of Table 3. The differences among the different models arise from the site energies associated with the T sites: model **I** gives the lowest site energy by 0.02 eV/formula unit over model **III**. Therefore, the Gd_5Si_4-type structures of $Gd_5(Si_xGe_{1-x})_4$ prefer to have Ge, the more electronegative atom of the two, in T1 sites. The electronegativity difference between Si and Ge manifests itself through the valence atomic orbital energies: $\epsilon_{4s}(Ge) < \epsilon_{3s}(Si)$ and $\epsilon_{4p}(Ge) \sim \epsilon_{3p}(Si)$ (see Table 3).

How this $Gd_5(Si_xGe_{1-x})_4$ series can tolerate such severe changes in T1−T1 bonding still remains as a puzzle despite recent theoretical efforts.[29] Nevertheless, a simple orbital rationale provides an important clue on why only T1−T1 dimers break rather than T2−T3 dimers during the Gd_5Si_4-type (LT) → $Gd_5Si_2Ge_2$-type (RT) transition (see Figure 4). In the Gd_5Si_4-type, the coordination environment surrounding each T1−T1 dimer has approximately "C_{2h}" (2/m) symmetry, which allows orbital mixing between σ_p and π^* (both gerade) or π and σ^* (both ungerade) molecular orbitals of the dimers. In contrast, the T2−T3 dimers in the slabs of the Gd_5Si_4-type has "D_{2h}" (mmm) symmetry. In this case no mixing is allowed among σ_p, π, π^*, and σ_p^* orbitals. It is the symmetry-allowed mixing between the π and σ^* molecular orbitals

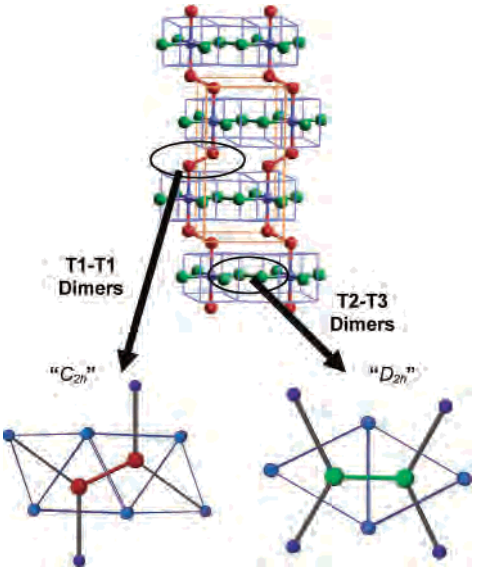

Figure 4. Approximate site symmetries for the two types of dimers in $Gd_5(Si_xGe_{1-x})_4$: (left) T1−T1 dimers have local C_{2h} symmetry; (right) T2−T3 dimers have approximate local D_{2h} symmetry. The color scheme is the same as in Figure 1.

of the T1−T1 dimers that leads to lower integrated COHP values for these interactions as compared to the T2−T3 bonds. Valence s−p orbital hybridization also contributes to the bond breaking phenomena in $Gd_5(Si_xGe_{1-x})_4$, and this effect is tied to the distribution of Si and Ge atoms among the T1, T2, and T3 sites. Since $\Delta_{sp}(Ge) > \Delta_{sp}(Si)$ ($\Delta_{sp} = \epsilon_{np} - \epsilon_{ns}$), there is greater s−p orbital hybridization in Si than in Ge, which makes the Si−Si σ^* orbital high in energy and reduces its symmetry-allowed mixing with the π orbital for the T1−T1 dimers. Therefore, Ge−Ge dimers will have a greater tendency to break during the phase transitions.

Structure Map. While compiling the lattice parameter data for various $Gd_5(Si_xGe_{1-x})_4$, we note that the b/a ratio vs c/a ratio plot can be a simple but powerful structure sorting map in this particular series. Kotur and co-workers[30] tried plotting a map on the basis of a/b and a/c ratios to distinguish binary Ln_5X_4 structures (Ln = lanthanides and Pu; X = Si,

(29) (a) Samolyuk, G. D.; Antropov, V. P. *J. Appl. Phys.* **2002**, *91*, 8540. (b) Harmon, B. N.; Antonov, V. N. *J. Appl. Phys.* **2002**, *91*, 9815. (c) Pecharsky, V. K.; Samolyuk, G. D.; Antropov, V. P.; Pecharsky, A. O.; Gschneidner, K. A., Jr. *J. Solid State Chem.* **2003**, *171*, 57.

(30) Kotur, B. Y.; Bodak, O. I.; Zavodnik, V. E. *Kristallografiya* **1986**, *31*, 868.

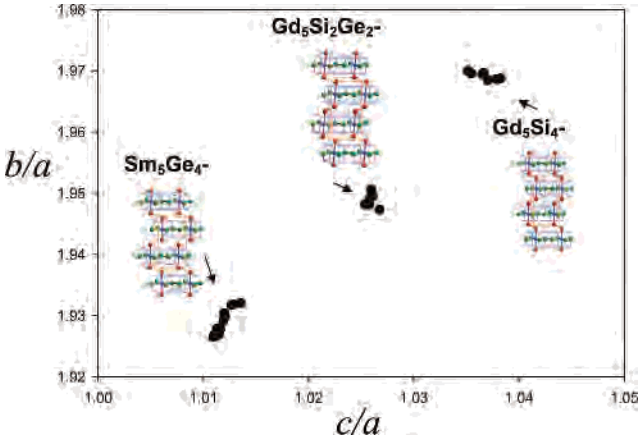

Figure 5. Structure map for 32 room-temperature structures of $Gd_5(Si_xGe_{1-x})_4$ using the lattice parameter ratios b/a and c/a.[6,7,9b,d] Each point corresponds to a different value of x, and the three regions are correspondingly labeled.

Ge, Sn, Pb, Rh, Ir, Pt, Au) for a broad spectrum of compounds, but they observed that the separation between different structure types is not evident. Within this specific system, such a map is effective and allows structural characterization on the basis of lattice constant determinations alone. Figure 5 illustrates the b/a ratio vs c/a ratio plot for 32 samples of the $Gd_5(Si_xGe_{1-x})_4$ series,[31] which shows the three structure types to be well separated. The b/a and c/a ratios are parameters to determine whether the lattice changes are isotropic or not. The most evident change in cell parameters occurs along the a direction. For example, the a parameter for Gd_5Ge_4 is about 3% greater than for Gd_5Si_4. This effect is due to the fact that T−T covalent bond formation or separation occurs parallel to the a direction. Whenever the two-dimensional $^{\infty}_{2}[Gd_5T_4]$ slabs are connected by (Si,Ge)−(Si,Ge) dimers, the c/a ratio increases. Therefore, the most dimer-rich structure type, Gd_5Si_4, has the highest c/a ratio. In contrast, the relative change in the b or c lengths is quite small, compared to a direction. The lattice parameter b of Gd_5Ge_4 is 0.6% greater than for Gd_5Si_4 while the lattice parameter c for Gd_5Ge_4 is 0.5% greater than for Gd_5Si_4. Although the difference in relative changes between the b and c direction is miniscule, it does help to separate the three structures as shown in Figure 5. The structure map shown here works especially well when the compounds are in the same series, like $Gd_5(Si_xGe_{1-x})_4$.

Recently we have found a new Ln_5T_4 series, $Gd_5(Ga_xGe_{1-x})_4$.[12d] One of its members, Gd_5GaGe_3, demonstrates an intermediate, orthorhombic structure between the Sm_5Ge_4-type and Gd_5Si_4-type, thereby opening up a new possibility of a new Ln_5T_4 series that can continuously vary the bond distance of the T1−T1 dimers between the slabs and allows us to study the relationship between the magnetic properties and the dimer separation between the slabs.[32]

Acknowledgment. The Ames Laboratory is operated by Iowa State University for the U.S. Department of Energy (DOE) under Contract No. W-7405-ENG-82. This work was supported by the Office of Basic Energy Sciences, Materials Science Division, of the U.S. DOE. The authors wish to thank Profs. Vitalij Pecharsky and Karl A. Gschneidner, Jr., for many fruitful discussions.

Supporting Information Available: An X-ray crystallographic file, in CIF format, containing information for $Gd_5(Si_xGe_{1-x})_4$, where $x = 0$, 0.11, 0.32, and 0.46, is available free of charge via the Internet at http://pubs.acs.org.

IC034941Z

(31) The cell parameters are from refs 9b,d and the current single crystal work. For the cell parameter b in monoclinic system, $b' = b\cos(\beta - 90°)$ is used instead because b' corresponds to b in the orthorhombic system, which also indicates the thickness of two $^{\infty}_{2}[Gd_5T_4]$ slabs in the $Gd_5(Si_xGe_{1-x})_4$ system.

(32) Pecharsky, V. K.; Holm, A.; Gschneidner, K. A., Jr.; Rink, R. *Phys. Rev. Lett.*, accepted for publication.